(BL5B)

Study of electronic structure and magnetic phase of Co film on oxygen-rich Cu(001)($\sqrt{2}$x2$\sqrt{2}$)R45°-O surface

Krishna G. Nath[1], Yuichi Haruyama[2] and Toyohiko Kinoshita[2]

[1]*The Graduate University for Advanced Studies, Okazaki 444-8585*

[2] *UVSOR facility, Institute for Molecular Science, Okazaki 444-8585*

In the present report, the magnetic properties and the reconstructed phase of ferromagnetic Co film on oxygen pre-adsorbed Cu(001) surface are shown. It is well known that the presence of molecules such as oxygen, sulfur etc. sometimes disturb to obtain the thin films with good quality. The reason may not be so clear, but disordered nature of the thin films and/or the substrates caused by the existence of the molecules probably seems to be one of the origins of the disturbance. It is interesting therefore to study the properties of ferromagnetic thin films grown on the ordered surface with the presence of the molecules. In order to study the magnetic stability of magnetic thin film on such substrate, we performed the LEED (low energy electron diffraction) and magnetic dichroism in photoemission spectroscopy experiments for the Co films grown on the oxygen adsorbed Cu substrate. The experiments were performed by using the modified XPS equipment; VG ESCALAB 220I-XL [1].

The Cu(001) substrate was cleaned by sputtering and annealing. Then the different amount of oxygen was exposed on the clean surface to obtain reconstructed surfaces. We observed two kinds of LEED patterns as a function of the amount of oxygen. At low amount (100L>) stage, the LEED pattern was not different from the clean 1x1 surface. At the higher amount (500L-1200L) stage, the superstructure Cu(001) ($\sqrt{2}$x2$\sqrt{2}$)R45°-O pattern was observed in accordance with the previous report [2]. However, no 'four-spot' or C(2x2) pattern reported previously [3] was observed in the present experiment. On these oxygen-rich Cu surfaces, 5ML of Co was evaporated.

Figure 1 shows the representative LEED photographs taken at different stages of experiment. As shown in the figure, the LEED is changed form ($\sqrt{2}$x2$\sqrt{2}$)R45° in (b) to c(2x2) in (c) upon depositing of 5ML Co. (d) shows the LEED pattern of the system O(3.2L)/Co(5ML)/Cu(001), where the oxygen was adsorbed on the clean Co film. The structures (c) and (d) seem to be same.

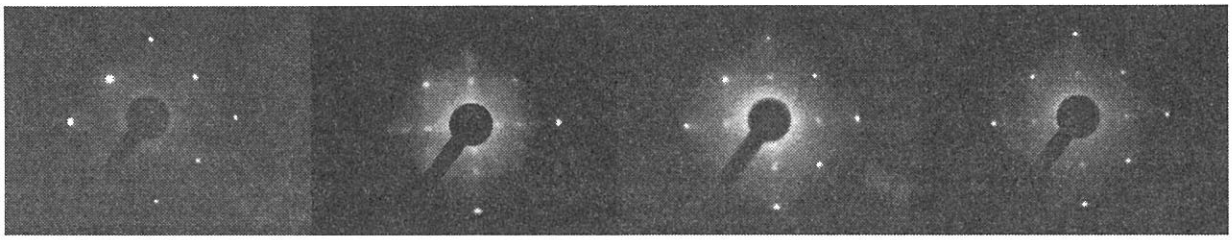

(a) (b) (c) (d)

Figure 1. LEED patterns of (a) clean Cu(001) at E_K=121eV, (b) O(1200L)/Cu(001), E_K=110eV, (c) Co(5ML)/O(1200L)/Cu(001), E_K=110eV, and (d) O(3.2L)/Co(5ML)/Cu(001), E_K=110eV .

Figure 2(a) shows the O 1s XPS spectra for the systems in Figs. 1 (b), (c) and (d), respectively. It is noticed that the binding energy between the Co/O/Cu (Fig.1(c)) and the O/Co/Cu (Fig.1(d)) is same in contrast to that of O/Cu (Fig. 1 (b)). It is concluded from the results of LEED and XPS that the oxygen in Co/O/Cu system comes out to the

topmost of the surface from the substrate. The amount is estimated to be the same coverage as that for 1L-coverage on clean Co film system. Binding energy position indicates that the bonding between the Co and floated oxygen is stronger than that of Cu-O. In Fig. 2(b), the MUDAD (magnetic dichroism in angular distribution by unpolarized light, here excited by MgKα) result of Co2$p_{3/2}$ is shown. As described previously [4], two spectra (upper panel) for opposite magnetization direction give an asymmetry (down panel), $(I_{M+}- I_{M-})/(I_{M+}+I_{M-})$. The presence of asymmetry signal (3%) means that the magnetic film with good quality can be grown on the oxygen pre-adsorbed substrate, namely even on the microscopically inhomogeneous (different domain exist on the oxygen-rich Cu) Cu-surface [2].

References

1. T. Kinoshita et al., J. Electron Spectrosc. Relat. Phenom. 92 (1998) 165.
2. F. M. Leibsle, Surface Science **337**, 51 (1995).
3. T. Fujita *et al.* Phys. Rev. B **54**, 2167 (1996).
4. M. Getzlaff *et al.*,Phys. Rev. Lett. **73**, 3030(1994)

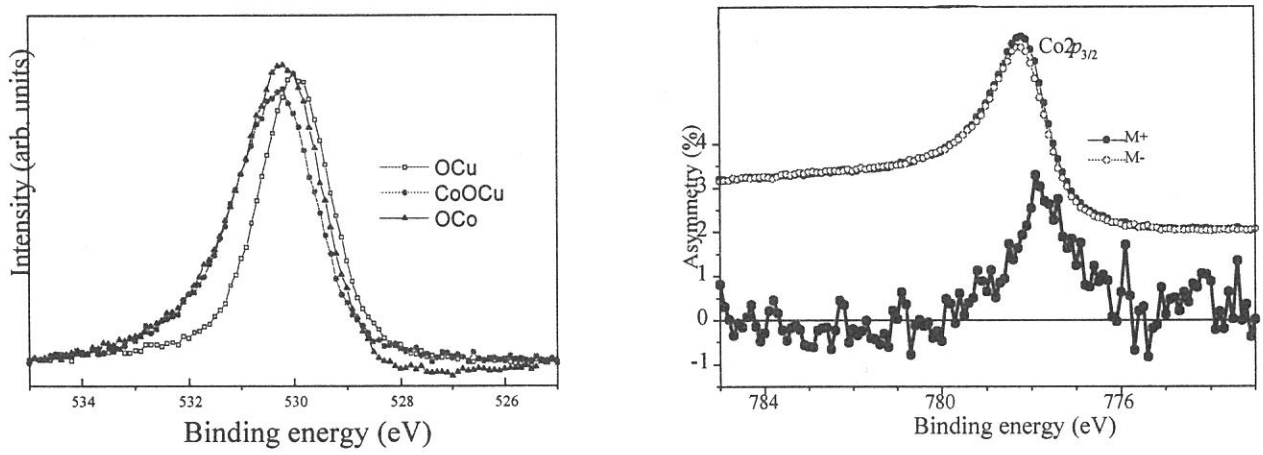

Figure 2. (a) O1s XPS spectra for three systems, O/Cu (open square), Co/O/Cu (solid circle) and O/Co/Cu (triangle). (b) MUDAD of Co2$p_{3/2}$ XPS for Co/O/Cu system.

(BL-5B)

Si-L Reflection Spectra of Si/CaF_2 Multilayers

Takeo EJIMA, Yuji KONDO and Makoto WATANABE

Research Inst. for Scientific Measurements, Tohoku Univ., Sendai 980-8577, JAPAN

Few years ago, we had measured total photoelectron yield (TEY) spectra of Si/CaF_2 multilayers around the Si-L edge changing angles of incidence. Recently, we have performed reflection measurements on the same samples. Preparation of the Si/CaF_2 multilayers are described in elsewhere [1]. The angle of incidence of the monochromatized light was changed from 0° to 88° in the measurements with its electric vector perpendicular to the plane of incidence.

The reflection spectra at angles of incidence between 60° and 88° for Si 185 Å /CaF_2 70 Å /Si(111) multilayer are shown in Figure 1. In the figure, solid lines represent results of the measurements, and dashed lines are results of tentative simulation using optical constants of crystalline Si and crystalline CaF_2 [2,3]. At angles of incidence between 0° and 60°, obtained signals are weak, therefore we could not distinguish the signals from backgrounds. With an increase of the angle, the spectral shapes change around the Si-L edge (100eV). The simulation is not satisfactory one to reproduce the measured spectral shapes well. We are now trying to find the optical constants which are able to reproduce both reflection and TEY spectra.

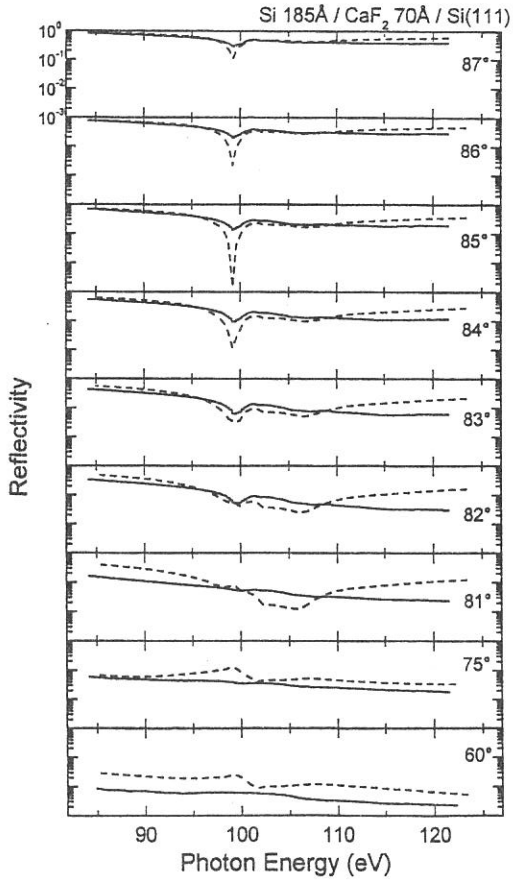

Figure 1: Reflection Spectra of Si 185Å /CaF_2 70Å/Si(111).

References

[1] T. Ejima, K. Ouchi, M. Watanabe: *Proc. of the 12th Int. Conf. on Vacuum Ultraviolet Radiation Physics*, San Francisco, 1998, to be published in J. Electron Spectros. Rel. Phenom.

[2] *Handbook of Optical Constants of Solids*, ed. E. D. Palik (Academic Press, 1985).

[3] B. L. Henke, P. Lee, T. J. Tanaka, R. L. Shimabukuro, B. K. Fujikawa: At. Data Nucl. Data Tables **27** (1982) 1.

(BL5B)

Absolute yield of exciton induced desorption from the surface of solid Ne

T. Hirayama[A*], T. Adachi[A], I. Arakawa[A,B], K. Mitsuke[B] and M. Sakurai[B]

[A]*Department of Physics, Gakushuin University, 1-5-1 Mejiro, Toshimaku, Tokyo 171-8588*
[B]*Institute for Molecular Science, Myodaiji, Okazaki 444-8585*

We have been studying the desorption of excited particles from the surface of rare gas solids (RGSs) induced by exciton creation using photon- and electron- stimulated desorption (PSD and ESD) techniques[1]. The mechanisms for the desorption of exited atoms in the excitonic energy region have been well established in these 10 years by measuring the kinetic energy, angular distribution, and excitation energy dependence using a synchrotron radiation[2, 3]. Absolute desorption yield can be an essential information for the quantitative understanding for the desorption dynamics. Hirayama et al. [4] first reported the absolute yield for exciton induced desorption of the metastable atoms from the surface of solid Ne. In the present study, we present the results for the total absolute yield for exciton induced desorption from the surface of solid Ne.

Experiments have been done at the beam line BL5B in UVSOR. The experimental setup is similar to the one used in our previous work[3] equipped with a quadrupole mass spectrometer (QMS400, ULVAC) in order to detect Ne molecules desorbed from the surface of solid Ne. Briefly, the sample substrate is a Pt(111) attached to the head of a rotatable liquid He cryostat installed in an UHV chamber (base pressure ~ 5×10^{-9} Pa). Absolute desorption yield has been estimated by the increase of Ne partial pressure measured by the quadrupole mass spectrometer, which is calibrated by using an extractor gauge (Lybolt). Pumping speed of a turbo molecular pump and the cryostat has been experimentally determined to be 0.16 m^3/s. Absolute number of the incident photon was measured using a photoelectric yield of Au plate as described in [4].

Figure 1 shows a wavelength dependence of the absolute desorption yield from the surface of solid Ne whose thickness is about 35 atomic monolayers. Positions of the first and second order bulk excitons (B1, B2) and the band gap energy (E_g) are marked in the figure. Only peak of bulk excitons has been appeared. Yield at the surface exciton (first order surface exciton, S1: 72.3 nm, $2p^53p$-type surface exciton, S': 65.4 nm) are less than our detection sensitivity (~ 0.1 atoms/photon). A broad peak at around 80 ~ 90 nm, where the excitation energy is below the lowest energy of the exciton creation (S1: 72.3 nm), is attributed to the desorption induced by the secondary electrons emitted from the platinum substrate. Unexpectedly large desorption yield (order of unity) can be explained by such a mechanism that the bulk exciton created near the surface, namely, second or third layer, desorbs via cavity ejection mechanism together with some ground state atoms around the excited atom. Further analysis is in progress.

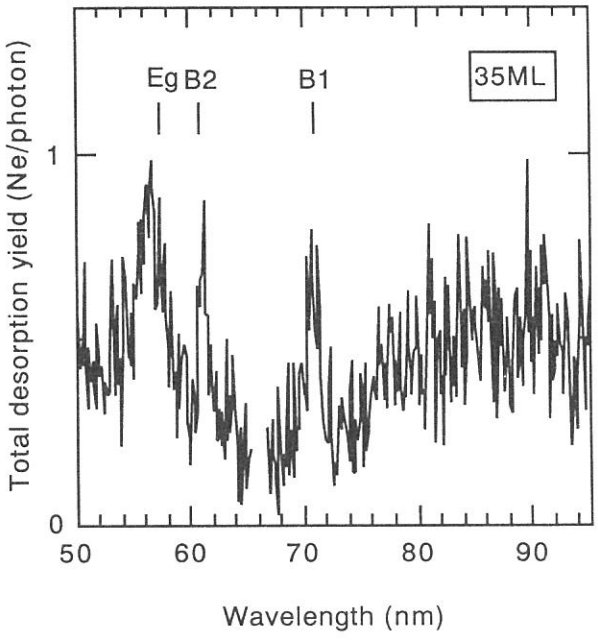

Fig.1. Excitation wavelength dependence of the absolute desorption yield from the surface of solid Ne.

References.

[1] I. Arakawa, in *Molecular Crystals and Liquid Crystals* (Gorden and Breach Science Publishers, New York, 1998), Vol. 314, p. 47.
[2] D. E. Weibel et al., Surface Science **283**, 204 (1993).
[3] I. Arakawa et al, Nucl. Instrum. Meth. Phys. Res. **B101**, 195 (1995).
[4] T. Hirayama et al., Surf. Sci. **390**, 266 (1997).

* Fax: 03-3987-6732, e-mail: takato.hirayama@gakushuin.ac.jp

(BL5B)

XUV radiation effects on back-thinned CCDs

S. Tsuneta, R. Kano, T. Sakao, K. Kobayashi[1], K. Kumagai

National Astronomical Observatory, 2-21-1 Osawa, Mitaka, Tokyo, 181, Japan
[1] *Department of Astronomy, School of Science, The University of Tokyo, Bunkyo-ku, Tokyo, 113, Japan*

Back-thinned CCDs have recently gained much attention as major detectors for astronomical applications, not only for ground-based observatories, but also for space-borne telescopes. For observations of the solar corona in the X/XUV wavelengths, back-thinned CCDs are well suited due to their high sensitivity to X/XUV light together with their high dynamic range.

As back-thinned CCDs started to be used in space, radiation hardness of back-thinned CCDs against incident X/XUV photons has become a major concern. EEV in UK and Site in US are only two major manufacturers currently producing large-format science-grade back-thinned CCDs. We have carried out experiments regarding XUV-radiation effects on several back-thinned CCDs purchased from EEV and SITe at UVSOR in the Institute of Molecular Science, Japan. Intense XUV beams from the synchrotron allows us to study, within a few days, effects of years of in-orbit XUV illumination from the sun. Systematic study on radiation hardness of back-thinned CCDs is done in the program for the first time.

We have illuminated both EEV and Site CCDs at 300 and 200Å. Fig. 1 shows the dark current level as a function of soft X-ray dose at 300Å. Fig. 2 shows the quantum efficiency (QE) with respect to the QE before the illumination. CCDs from EEV have turned out to be significantly robust against XUV photons at 200 and 300 angstroms. EEV CCDs show slight, or even marginal, increase in the dark current level after XUV illumination equivalent to several years of solar observations from space, while maintaining high quantum efficiency (higher than 0.5). On the other hand, Site CCDs have experienced significant increase in dark current level, and decrease in QE. We also performed the experiment at 50Å, and obtained essentially the same result.

The degradation both in dark current level and in the quantum efficiency is related to the sensitive back-surface of the CCDs. CCDs silicon substrate is mechanically and chemically etched to thickness of about 10 microns, and the silicon-silicon-dioxide layer has many intermediate traps. Although the degradation appears to be related to the intermediate states, polarization of the silicon-silicon-dioxide interface due to soft X-ray irradiation, and the resultant change in the internal potential profile, the physical mechanism is not completely understood, and is being discussed with the manufacturers. The difference in performance between EEV and Site is related to that in method of annealing. A full paper for the experiment is being prepared.

As a practical side, this experiment serves to choose the best possible CCD device for the Solar-B spacecraft. Solar-B is scheduled to be launched in the year 2004 by the Institute of Space and Astronautical Science (ISAS). The X-ray telescope (XRT) is developed under Japan-U.S. collaboration. The Japanese XRT team is responsible for the development of the CCD camera, together with associated electronics.

References (published in FY1998):

T. Sakao, R. Kano, K. Kobayashi, and S. Tsuneta, 1999, XUV radiation effects on back-thinned CCDs, in Proc. International Symposium on Solid State Detectors.

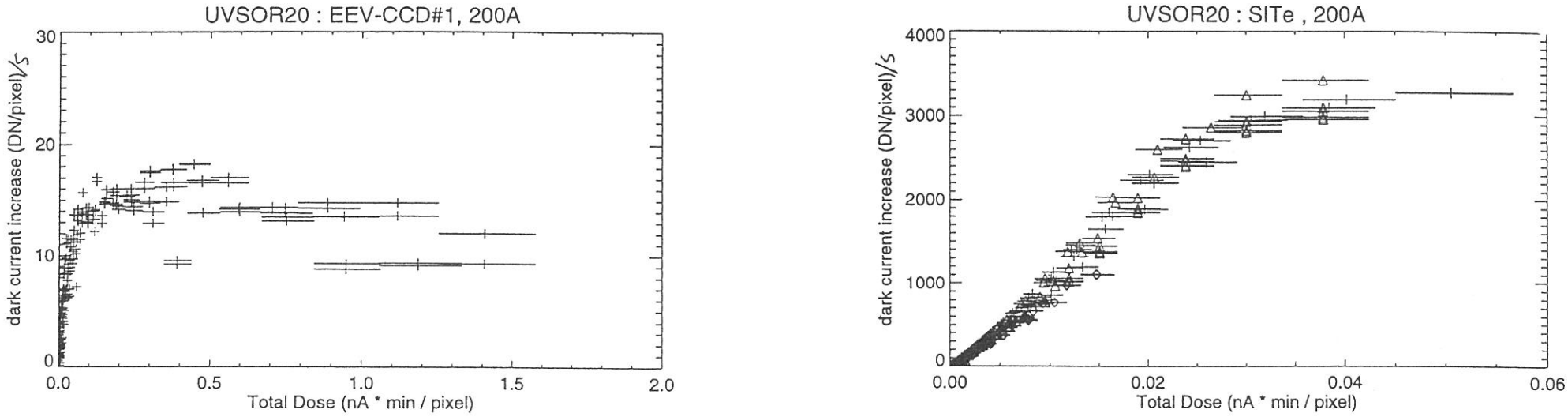

Figure 1: Dark current level as a function of the soft X-ray dose at 200Å; (left) EEV CCD, (right) Site CCD.

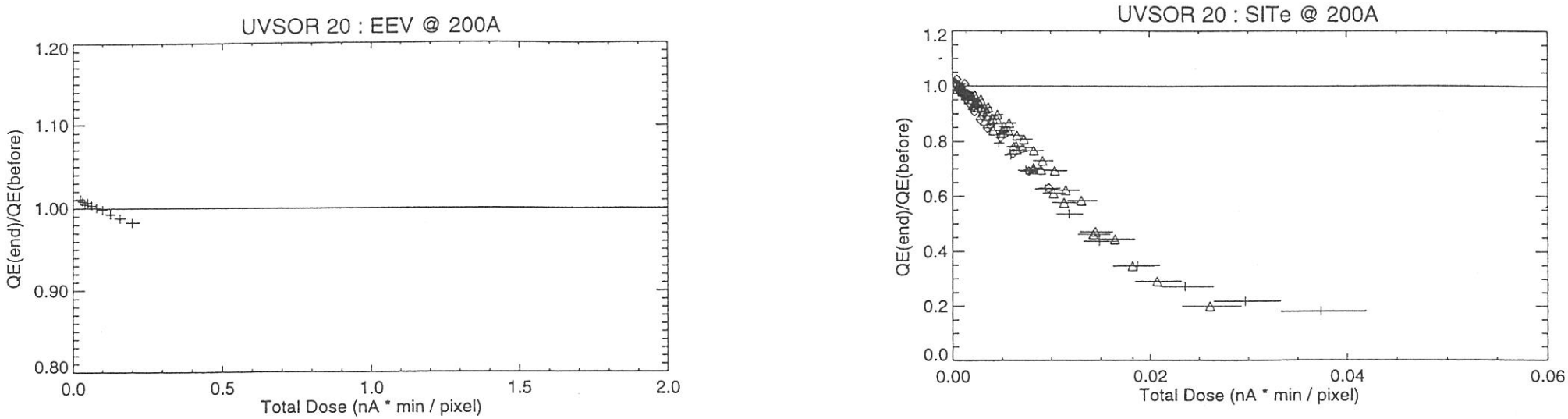

Figure 2: Relative quantum efficiency as a function of the soft X-ray dose at 200Å; (left) EEV CCD, (right) Site CCD.

(BL5B)

Electronic structures of organic salts (DI-DCNQI)$_2$M (M = Cu and Ag) using photoelectron spectromicroscopy

Yuichi Haruyama,[A] Krishna G. Nath,[B] Shin-ichi Kimura,[C] Yüksel Ufuktepe,[D]
Toyohiko Kinoshita,[A,E] Ko-ichi Hiraki[F] and Kazushi Kanoda[G]

[A]*UVSOR Facility, Institute for Molecular Science, Okazaki 444-8585, Japan*

[B]*Department of Structural Molecular Science, The Graduate University for Advanced Studies, Okazaki 444-8585, Japan*

[C]*Division of Structural Science, Graduate School of Science and Technology, Kobe University, Kobe 657-8501, Japan*

[D]*Physics Department, University of Cukurova, 01330 Adana, Turkey*

[E]*Institute for Solid State Physics, University of Tokyo, Tokyo 106-8666, Japan*

[F]*Department of Physics, Gakushuin University, Tokyo 171-8588, Japan*

[G]*Department of Applied Physics, University of Tokyo, Tokyo 113-8656, Japan*

The crystal structures of (DI-DCNQI)$_2$M (M=Cu, Ag), where DI-DCNQI is 2,5-diiodo-*N*,*N*'-dicyanoquinonediimine, are isostructural with a space group $I4_1/a$, whereas the physical properties are quite different from each other. In the electrical resistance [1], (DI-DCNQI)$_2$Cu (abbreviated DI-Cu) shows metallic conductivity down to low temperature, on the other hand, (DI-DCNQI)$_2$Ag (DI-Ag) shows semiconducting nature with a gap of 490K. The difference in the physical properties is considered to arise from the *d* band position of M ion. Although the photoemission is a direct method to investigate these electronic structures, the photoemission study for the single crystals DI-Cu and DI-Ag has not been performed so far. The reason is that the size of these single crystals is not large enough to carry out the photoemission experiments. However, photoelectron spectromicroscopy apparatus can do the experiment. Therefore, we have measured the photoemission spectra for DI-Cu and DI-Ag using the photoelectron spectromicroscopy [2].

Photoemission experiments were carried out by using a conventional UHV system (FISONS, ESCALAB-220i-XL) at a base pressure of 2×10^{-8} Pa [2]. Total instrumental energy resolution was 0.3~0.6 eV full width at half maximum (FWHM), depending on the photon energy ($h\nu$) in the energy range of 30~200 eV. Needlelike shaped single crystals of DI-Cu and DI-Ag were synthesized by electrochemical reduction [1]. Figure 1 shows the photoelectron image of DI-Ag excited by AlKα light of $h\nu$=1486.6 eV. The I $3d_{5/2}$ photoelectrons at E_B= 620 eV were collected. The typical sample size used here was less than $\phi100\times1000\mu m^2$. These samples were characterized by x-ray diffraction, electrical resistance, magnetic susceptibility and NMR measurements [1]. The clean surface was obtained by scraping the sample surface using an edge of a razor. The cleanliness was confirmed by x-ray photoemission spectroscopy for the absence of extra features arising from the contaminations.

Figure 2(a) shows the photoemission spectra of DI-Cu and DI-Ag, respectively. The detection area of the photoemission spectra was 50μm, which is smaller than the sample size. For DI-Cu, five features in this valence band region are observed at ~0.5, 3.2, 4.0, 6.5 and 9.0 eV labeled A, B, C, D and E, respectively. It is recognized that from the photon energy dependence of the photoemission spectra that the features A, C and D are predominantly derived from N and C 2*p* states, and the feature B is from Cu 3*d* states [3]. For DI-Ag, five features in this valence band region are observed at ~0.5, 4.0, 5.2, 6.6 and 9.0 eV labeled by F, G, H, I and J, respectively. The features F, G and I are predominantly derived from N and C 2*p* states, and the feature H is from Ag 4*d* states [3]. It is obvious that the Ag 4*d* states have much deeper than the Cu 3*d* states. In addition,

as shown in Figure 2(b), the spectral feature above ~0.5 eV for DI-Cu is larger than that for DI-Ag. This is probably due to the contribution of the Cu 3*d* states. The tail of the Cu 3*d* states seems to reach near the Fermi level. These results indicate that the *pπ-d* hybridization at the Fermi level between the M ions and the N atoms of the DCNQI molecules for DI-Cu is large as compared with that for DI-Ag. The tendencies of the position of the metal M *d* states are consistent with the band calculation [4]. However, the position of features A and F assigned to the pπ orbitals (LUMO) is not consistent with the band calculation [4]. This shows the importance of the electron correlation.

References

[1] K. Hiraki and K. Kanoda, Phys. Rev. **B 54**(1996)17276.

[2] T. Kinoshita, K. G. Nath, Y. Haruyama, M. Watanabe, S. Yagi, S. Kimura, and A. Fanelsa, J. Electron Spectrosc. Relat. Phenom. **92**(1998)165; T. Kinoshita, K. G. Nath, M. Watanabe, S. Yagi, S. Kimura, and A. Fanelsa, UVSOR Activity Report 1996, p.154.

[3] Y. Haruyama, K. G. Nath, S. Kimura, Y. Ufuktepe, T. Kinoshita, K. Hiraki and K. Kanoda, Solid State Commun. in press.

[4] T. Miyazaki and K. Terakura, Phys. Rev. **B 54**(1996)10452.

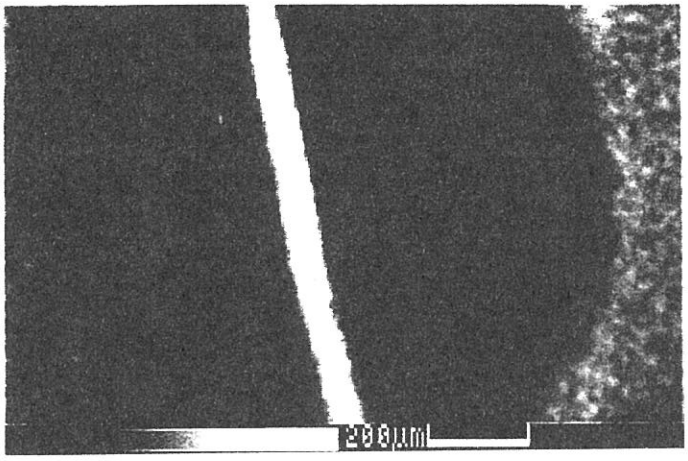

Figure 1. Photoelectron image of $(DI\text{-}DCNQI)_2Ag$ excited by AlKα light of $h\nu$= 1486.6 eV. The I $3d_{5/2}$ electrons at E_B = 620 eV were collected.

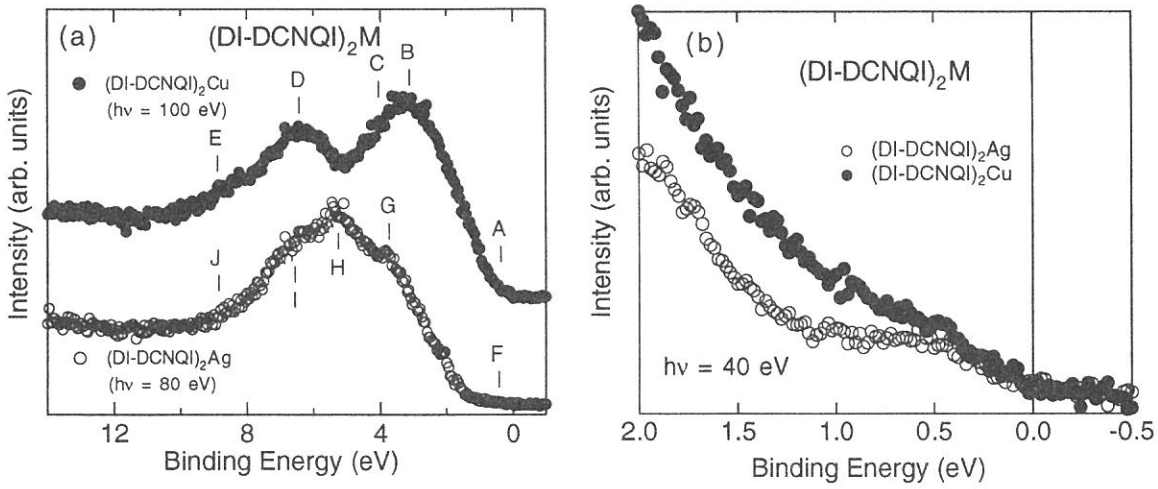

Figure 2. The photoemission spectra of $(DI\text{-}DCNQI)_2Cu$ and $(DI\text{-}DCNQI)_2Ag$ (a) in the whole valence band region (b) near the Fermi level. The detection area was 50μm.

(BL5B)

Measurement of absolute efficiency for MCP onboard Mars orbiter by using pure-calibrated EUV beam

Masato Nakamura[1], Yoshiyuki Takizawa[2], Ichiro Yoshikawa[3]
Atsushi Yamazaki[1], Kei Shiomi[1], and Etsushi Ohyama[1]
[1] *Department of Earth and Planetary Science, Univ. of Tokyo, Bunkyo-ku, Tokyo 113-0033*
[2] *The Institute of Physical and Chemical Research, Wako, Saitama 351-0198*
[3] *Institute of Space and Astronautical Science, Sagamihara, Kanagawa 229-8510*

As one of the calibrations for the sensitivity characteristics of the eXtreme Ultra-Violet Scanner (XUV) onboard the Mars orbiter *NOZOMI*, the object of this experiment is to measure the quantum efficiency of the same-type MCPs as XUV on flight at the 304 Å line. For this purpose, during this whole machine time an Al/Mg/Al (744 Å/3958 Å/747 Å) filter is installed on the SOR beam's entrance to eliminate the multi-order lines from the 304 Å line with PGM35/36. As the usual detectors which are set on the outer rotation stage of the goniometer, we use our position-sensitive MCPs when using PGM36 and the photo diode when PGM35.

We investigate the purity of the 304 Å line through the Al/Mg/Al filter in the following two ways. At first, we judge the purity from the consistency between the transmittance of an Al/Mg/Al (744 Å/3958 Å/747 Å) filter and an Al/Sn (1608 Å/500 Å) filter for the continuous lines at UVSOR and that for the particular lines at the University of Tokyo EUV facilities. The latter is measured for the emission lines of the gas (He, Ne) with the discharge light source. Fig.1 shows the transmittance profiles of the two filters measured at UVSOR and University of Tokyo. It is clear that both profiles of each filter are consistent in the wavelength region of 250-500 Å. Second, we investigate the dispersion of the 304 Å line with PGM35 by using our grating for experiments on the X-Y stage of the goniometer. The result shows that no contamination of the 152 Å line (the second-order line) and the 76 Å line (the fourth-order line) exists. Not exactly, we seem that the contamination of the 38 Å line (the eighth-order line) exists much a little.(Fig.2) But even if it should exist, the result of the transmittance analysis turn out that the degree of the contamination almost can be neglected. We interpret from the two results that the pure 304 Å line can be introduced through the Al/Mg/Al filter by using PGM35/36.

With the available pure 304 Å line, we measure the quantum efficiency of the XUV-type MCPs which are set on the X-Y stage of the goniometer, and our position-sensitive MCPs. The quantum efficiency is calculated by the rate of the MCPs count to the electron yield of the photo diode which is absolutely calibrated. Table1 shows that the quantum efficiency of

the XUV-type MCPs is 11.3%(HV:-2.90kV). The position-sensitive MCPs is 9.2%.

As the next step, in addition to the 304Å line (He II emission), we plan to measure the quantum efficiency at the 584Å line (HeI emission), which is another observational object of XUV. Then the purity of 584Å line is essential, and must be investigated for the next machine time.

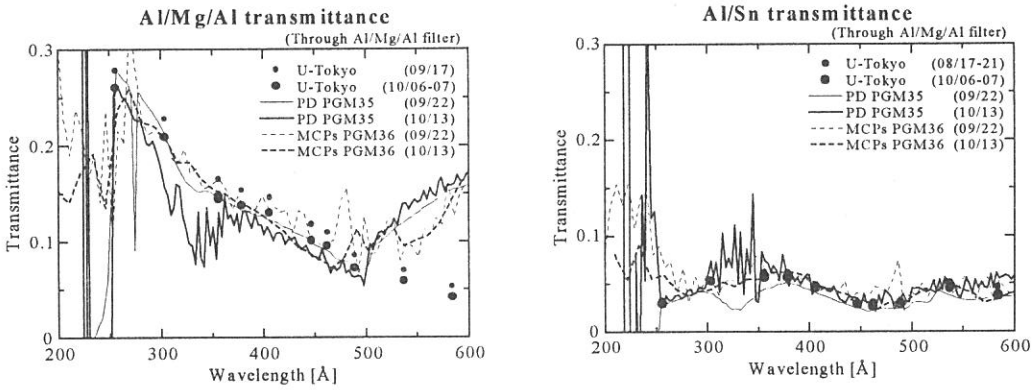

Fig.1 The transmittance profiles of an Al/Mg/Al(744Å/3958Å/747Å) filter and an Al/Sn(1608Å/500Å) filter. The solid and dashed lines show the measurement at UVSOR, and the solid circles show those at the University of Tokyo EUV facilities.

Fig.2 The dispersion of the 304Å line detected by the position-sensitive MCPs.

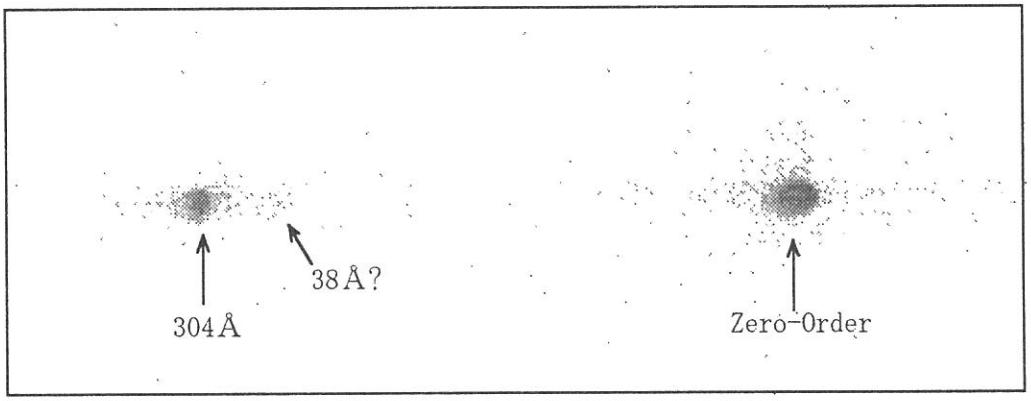

Table 1 The quantum efficiency of the XUV-type MCPs at the 304Å line.

High Voltage	The quantum efficiency
-2.65kV	9.1%
-2.70kV	9.9%
-2.80kV	10.8%
-2.90kV	11.3%
-3.00kV	11.7%
-3.10kV	11.9%

(BL5B)

Soft X-Ray Reflectances of Novel Oxide Multilayer Structures Fabricated by Atomic Layer Deposition

Hiroshi Kumagai, Katsumi Midorikawa, Hiroko Matsuyama[A], Hidehiko Asahi[A] and Minoru Obara[A]

Laser Technology Laboratory,
The Institute of Physical and Chemical Research (RIKEN),
2-1 Hirosawa, Wako, Saitama 351-0198, Japan
[A] *Electrical Engineering, Faculty of Science and Technology, Keio University,*
3-14-1 Hiyoshi, Kohoku-ku, Yokohama 223-0061, Japan.

Development of high-performance normal-incidence multilayer optics for the water-window wavelength region between the oxygen and carbon K absorption edges at 2.33 and 4.36 nm, respectively, where water is relatively transmissive and organic materials are absorptive, has been a technical challenge of great interest. The extremely small periods (1.2-2.2 nm) of soft-X-ray reflectors require very rigorous specifications to be met with respect to interface roughness and interlayer mixing, because interface roughness on an atomic scale has a substantial effect on soft-X-ray reflectance. Therefore, the reflectances achieved at these wavelengths are very low.

The authors have proposed the use of a novel metal oxide multilayer, whose material combination is the same as that used in free electron lasers, for soft-X-ray reflectors at water-window wavelengths,[1,2] because an oxide multilayer can prevent from forming an alloy at the interface, and the absorption of oxygen in oxides is negligible at the water-window wavelengths; moreover, the metal oxide multilayer can be fabricated by the atomic layer deposition or atomic layer epitaxy technique. These techniques can be used to control surfaces on an atomic scale by sequentially dosing the surface with appropriate chemical precursors and then promoting surface chemical reactions which are inherently self-limiting. We have found that the self-limiting adsorption mechanism works in the fabrication of oxide thin films such as aluminum oxide and titanium oxide.[3-5]

We report here on reflectance performances of novel metal oxide multilayers of titanium oxide and aluminum oxide using monochromatized synchrotron radiation (SR) from the beamline 5B of the 750-MeV electron storage ring located at the Ultraviolet Synchrotron Radiation Facility (UVSOR).

Figure 1 shows the experimental results of wavelength dependence on reflectances of the aluminum oxide/titanium oxide multilayer fabricated by the atomic layer deposition method of controlled growth with sequential surface chemical reactions. A high reflectance (s-polarization) of 33.4% at the wavelength of 2.734 nm and an incident angle of 71.8° from the normal incidence are demonstrated in the 20-period structure of d=4.43nm. A reflectance (s-polarization) over 15% at the wavelength of 2.734 nm and an incident angle of 58.5° from the normal incidence are demonstrated in the 40-period structure of d=2.62 nm.

Figure 2 shows comparisons between measured reflectances, calculations with and without surface roughness. In the cases of #2 and #3, experimental reflectances are almost the same as the calculations without roughness. For the case #1, whose period is 2.17 nm, the measured reflectance is close to the calculation with roughness. The descrepency between experimental and calculated reflectances might arise from the surface/interface roughnesses and interlayer mixing and so on.

This work was supported by the Joint Studies Program (1998) of the Institute for Molecular Science.

References

1) H. Kumagai, K. Toyoda, K. Kobayashi, M. Obara and Y. Iimura, Appl. Phys. Lett. 70, 2338 (1997).
2) H. Kumagai, M. Matsumoto, Y. Kawamura, K. Toyoda and M. Obara, Jpn. J. Appl. Phys. 33, 7086 (1994).
3) H. Kumagai, K. Toyoda, M. Matsumoto and M. Obara, Jpn. J. Appl. Phys. 32, 6137 (1993).

4) H. Kumagai and K. Toyoda, Appl. Surf. Sci. 82/83, 481 (1994).
5) H. Kumagai, M. Matsumoto, K. Toyoda, M. Obara and M. Suzuki, Thin Solid Films 263, 47 (1995).

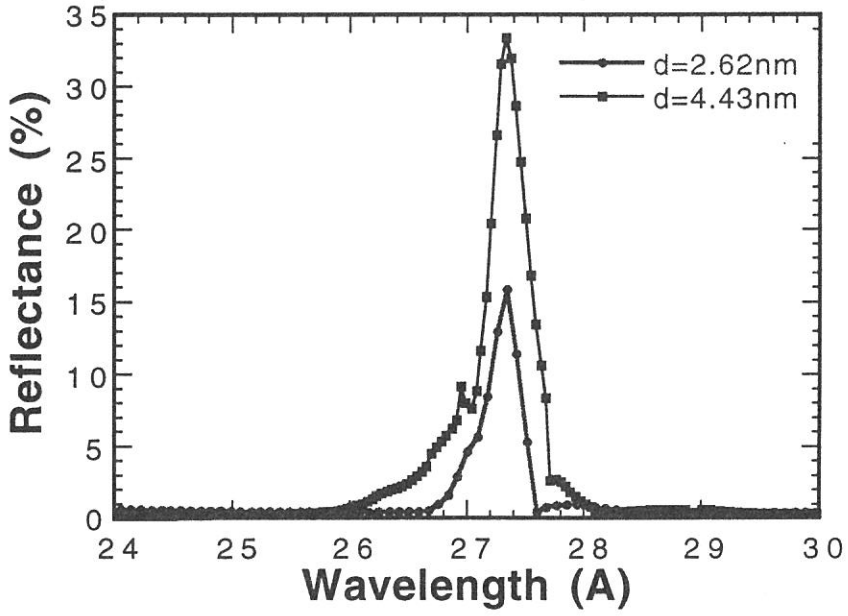

Fig.1 Plots of wavelength dependence on reflectances of the aluminum oxide/titanium oxide multilayer with different periods fabricated by the atomic layer deposition method of controlled growth with sequential surface chemical reactions.

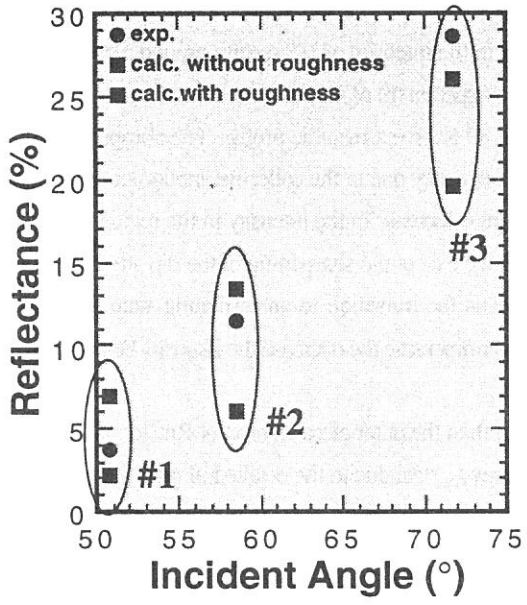

	#1	#2	#3
incident angle	50.8°	58.5°	71.8°
period	2.17nm	2.62nm	4.43nm
number of periods	40	40	20
roughness	0.37nm	0.37nm	0.373nm
substrate	Si(100)	Si(100)	Si(100)

Fig.2 Comparisons between measured reflectances, calculations with and without surface roughness. The wavelength is 2.742 nm which corresponds to Ti Lα.